Climate Dynamics (1999) 15:251–268

T. Fichefet · M. A. Morales Maqueda

Modelling the influence of snow accumulation and snow-ice formation on the seasonal cycle of the Antarctic sea-ice cover

Received: 30 June 1997/Accepted: 2 October 1998

Abstract Recent observational and numerical studies of the maritime snow cover in the Antarctic suggest that snow on top of sea ice plays a major role in shaping the seasonal growth and decay of the ice pack in the Southern Ocean. Here, we make a quantitative assessment of the importance of snow accumulation in controlling the seasonal cycle of the ice cover with a coupled snow–sea-ice–upper-ocean model. The model takes into account snow and ice sublimation and snow deposition by condensation. A parametrisation of the formation of snow ice (ice resulting from the freezing of a mixture of snow and seawater produced by flooding of the ice floes) is also included. Experiments on the sensitivity of the snow–sea-ice system to variations in the sublimation/condensation rate, the precipitation rate, and the amount of snowfall transported by the wind into leads are discussed. Although we focus on the model response in the Southern Hemisphere, results for the Arctic are also discussed in some cases to highlight the relative importance of the processes under study in both hemispheres. It is found that the snow loss by sublimation can account for the removal of 0.45 m of snow per year in the Antarctic and that this loss significantly affects the total volume of snow ice. A precipitation decrease of 50% is conducive to large reductions in the Antarctic snow and snow-ice volumes, but it leads only to an 8% decrease in the annual mean ice volume. The Southern Ocean ice pack is more sensitive to increases in precipitation. For precipitation rates 1.5 times larger than the control ones, the annual mean snow, ice, and snow-ice volumes augment by 30, 20, and 180%, respectively. It is also found that the transfer to the ocean of as much as 50% of the precipitating snow as a result of wind transport has almost negligible effects on the total ice volume. All the experiments exhibit a marked geographical contrast in the ice-cover response, with a much larger sensitivity in the western sector of the Southern Ocean than in the eastern sector. Our results suggest that snow-related processes are of secondary importance for determining the sensitivity of the Arctic sea ice to environmental changes but that these processes could have an important part to play in the response of the Antarctic sea-ice cover to future, or current, climatic changes.

T. Fichefet (✉) · M. A. Morales Maqueda[1]
Institut d'Astronomie et de Géophysique G. Lemaître,
Université Catholique de Louvain,
B-1348 Louvain-la-Neuve, Belgium
e-mail: fichefet@astr.ucl.ac.be

Present address:
[1]Department of Mathematics, Keele University, Staffordshire,
ST5 5BG, United Kingdom

1 Introduction

Snow that accumulates on top of sea ice can significantly alter the physical behaviour of the sea-ice cover and, therefore, introduce appreciable modifications in the exchanges of heat, momentum, freshwater, and salt between ocean, sea ice, and atmosphere. These modifications, in turn, can impact on air temperatures (Ledley 1991), water-mass formation (Gordon and Huber 1990), and marine biology (Arrigo et al. 1997).

A number of snow processes compete against each other in shaping the seasonal cycle of the sea-ice cover. Because of its low thermal conductivity, the snow cap acts as an insulating blanket that curtails the conduction of heat from the ice–ocean interface to the surface, thus slowing down basal ice growth. As a result, during autumn and winter, snow-covered ice tends to be warmer and thinner than snow–free ice. Concurrently, the air layer above the snow–ice cover tends to be colder and the mixed layer underneath tends to be fresher (due to the decrease in the rate of brine rejection). The importance of this thermal effect of snow depends on the ratio of snow and ice thicknesses. If the snow

thickness is small relative to the ice thickness, the internal conductive heat flux will be barely affected by the presence of snow. On the contrary, if the snow thickness is comparable to the ice thickness, heat conduction will be drastically reduced (a 0.3-m-thick snow layer over 2 m of ice halves the conductive heat flux as compared to that through bare ice of the same thickness). Furthermore, owing to its high albedo, the snow cover acts as a protective screen against the incoming shortwave radiation, retarding or even frustrating the onset of melting. The fact that the mass of snow has itself to melt away before any melting of the ice underneath occurs introduces a further delay in the beginning of ice melting, although this deferring mechanism is usually less important than the one due to the albedo because of the low volumetric latent heat of fusion of snow. For these reasons, during spring and summer, the snow cover tends to preserve the ice cooler and thicker, to maintain air temperatures lower, and to keep upper-ocean waters saltier than they would be in the absence of snow.

Snow can also actively contribute to the thickening of ice via the process of snow-ice formation. Snow ice is the product of freezing of water-soaked snow resulting from the infiltration of rain, meltwater, or seawater above the snow-ice interface. In spring and summer, snow ice can form as superimposed ice by freezing of slush (a mixture of rain or melted snow and snow). Formation of snow ice from mixing of seawater and snow can arise all along the year. Mechanisms for soaking the snow cover with seawater are waves breaking against ice floes and promotion of negative ice freeboard, which allows seawater to penetrate the snow depressed under the waterline. Negative freeboards come about as a consequence of ice ridging and deformation or by alteration of the isostatic balance of the ice floes under an excessive snow load. In this case, once snow-ice formation has been initiated, the maintenance of the process depends upon the ratio between snow-accumulation and basal ice-accretion rates, with snow-ice formation being likely to occur over thin ice subjected to heavy snowfall.

The impact of snow accumulation on the sea-ice cover depends on the timing and intensity of snow deposition and ablation along the seasonal cycle and on the characteristics of the ice cover (its thickness, in particular) upon which snow accumulates. The spatiotemporal patterns of snow accumulation and melting over sea ice exhibit strong hemispheric contrasts. In most of the Arctic Ocean, the snow cover is seasonal, although satellite imagery has revealed substantial interannual variability in snow extent (Scharfen et al. 1987). The drastic increase in shortwave radiation during May and June leads to a rapid melting of snow that usually results in the disappearance of the snow cover by the middle of July. Around mid-August, fresh snow begins to accumulate and subsequent fall and winter precipitation fosters a gentle growth of the snow cover. Measurements of snow depth reach near 0.2 m by the end of autumn (Hanson 1965) and peak at 0.3–0.4 m in April and May (Vowinckel and Orvig 1970). In the Antarctic, perennial sea ice is commonly covered by permanent snow. The thick snow cover (0.53 m, on average) of the western Weddell Sea has been shown to be a multiyear one (Eicken et al. 1994). Maps of snow distribution generated from remote sensing data show that, in the central Weddell Sea, snow remains relatively deep (0.17 m, on average) throughout austral spring and summer (Arrigo et al. 1997). Deep snow, ranging from 0.17 to 1.98 m, has also been observed on floes in the eastern Ross Sea, the Amundsen Sea, and the Bellingshausen Sea in February, with evidence of more than one winter accumulation (Jeffries et al. 1994a, b). Finally, satellite observations of coastal patches of multiyear ice in the Indian and western Pacific sectors of the Southern Ocean indicate that a snow cover of depth averaging between 0.13 and 0.17 m persists in these regions at the height of the summer season (Arrigo et al. 1997).

The difference between the maritime snow covers in the Arctic and Antarctic is a consequence of disparities in the surface energy budgets of both regions. In the Arctic, the ablation season is characterised by very active surface melting, as demonstrated by both observations (e.g. Hanson 1965) and modelling studies (e.g. Maykut and Untersteiner 1971). By contrast, surface melting in the Southern Ocean is very rare, although snow melting and melt ponding have been observed over land-fast ice near Prince Olav coast (Takahashi 1960) and over multiyear ice in the northwest region of the Weddell Sea (P Wadhams personal communication), and signs of summer snow melting in the Bellingshausen and Amundsen Seas have also been reported (Jeffries et al. 1997). Andreas and Ackley (1982) provide evidence that, in the Southern Ocean, the turbulent heat transfer to the atmosphere dominates the net radiative heat gain at the surface, thus precluding snow/ice melting. Strong winds, with typical velocities of $10\,m\,s^{-1}$ (60 to 100% larger than Arctic wind speeds), and low relative humidities (60% versus 75% or more in the Arctic) appear to be the main mechanisms driving the enhancement of surface turbulent heat fluxes (especially the latent heat flux) in the Antarctic.

The fact that the Arctic sea-ice cover is primarily formed by fairly thick ice (3 m on average in the central Arctic; Bourke and Garrett 1987) suggests that the impact of the snow cover on the internal conductive heat flux is relatively weak there and that snow-ice formation is uncommon. (In the Baltic Sea, however, sea ice does not exceed 1 m in thickness and snow ice can count to one third of the total ice thickness; Leppäranta 1983.) In addition, the seasonality of the Arctic snow cover implies that the albedo effect of snow is not operational during part of the summer season. One would therefore presume that the sensitivity of the Arctic ice pack to variations in snow deposition is

weak. Modelling studies suggest, indeed, that perturbations in the annual snowfall rate less than about twice the observed value have only a modest influence on the seasonal cycle of sea ice in the Arctic (Maykut and Untersteiner 1971; Semtner 1976; Harvey 1988; Ledley 1991, 1993; Holland et al. 1993; Ebert and Curry 1993). In contrast, the snow cover is expected to play a more vital role in the Southern Ocean. Since the Antarctic ice pack is comparatively thin (less than 1 m, on average; Budd 1991), it can be anticipated that the insulating effect of the snow cover exerts a strong control on the basal ice growth and that snow-ice formation occurs over large areas. Furthermore, the persistence of the snow cap throughout the year has two important consequences: first, the albedo effect is active during the whole length of the ablation season; second, snow over multiyear ice is itself multiyear and hence relatively thick. The numerical experiments conducted by Owens and Lemke (1990), Stössel et al. (1990), Eicken et al. (1995), and Fichefet and Morales Maqueda (1997) confirm that the Antarctic sea ice is remarkably sensitive to the presence or absence of snow and to changes in the rate of snowfall.

The thrust of this study is to evaluate the influence of snow accumulation and snow-ice formation on the seasonal cycle of sea ice. To this end, we have carried out a series of numerical experiments with a global model of the coupled snow–sea-ice–upper-ocean system. These experiments are aimed at estimating the response of the Arctic and Antarctic ice packs to alterations in the snow-accumulation rate. Such alterations can originate from perturbations in either the surface evaporative flux, the precipitation rate, or the loss of snow to the ocean by the drifting snow mechanism, a process that, according to Eicken et al. (1994), might be important in the Antarctic. The model explicitly computes the surface sublimation/condensation rate, and it determines the fraction of precipitation falling as snow from climatological data. Albeit simple, the parametrisations of snow and sea-ice processes included in the model are deemed sufficient for an assessment of snow–ice interactions in the large scale. In particular, the insulating, albedo, and mass effects of snow upon ice and the formation of snow-ice are accounted for. We focus our study on the sea-ice cover of the Southern Ocean, where snow-related processes are likely to be the most relevant. Nevertheless, in order to highlight the physical and climatic repercussions of the processes under investigation, the response of the Arctic ice pack is also examined in certain cases.

The rest of the work is organised as follows. Section 2 provides a brief description of the model. The model sensitivity to prescribed perturbations in the sublimation/condensation rate, the precipitation rate, and the amount of snowfall blown into leads by the wind is investigated in Sect. 3. Section 4 closes the paper with a summary and some concluding remarks.

2 Model description

The large-scale snow–sea-ice–upper-ocean model used in our experiments has been described in detail by Fichefet and Morales Maqueda (1997; hereafter referred to as FMM). Several modifications have been introduced, however, to better portray energy and mass exchanges at the surface of the snow–ice system and to improve the simulation of snow-ice formation. To assist the reader, we provide here a succinct description of the coupled model and a complete discussion of the novelties introduced into the snow–sea-ice component for this study.

The snow–sea-ice model is a thermodynamic–dynamic one. Sensible heat storage and vertical heat conduction within snow and ice are determined by a three-layer model (one layer for snow and two layers for ice). The storage of latent heat inside the ice resulting from the trapping of shortwave radiation by brine pockets is taken into account. The model also allows for the presence of leads within the ice pack. Vertical and lateral growth/decay rates are obtained from the prognostic energy budgets at both the bottom and surface boundaries of the snow–ice cover and in leads.

The parametrisation of the surface albedo is that of Shine and Henderson-Sellers (1985), combined with the modifications for clear and overcast conditions recommended by Grenfell and Perovich (1984). This albedo parametrisation takes into consideration the state of the surface (frozen or melting) and the thickness of the snow and ice covers. As most sea-ice models, ours drains away all of the summer meltwater. However, the reduction in surface albedo due to the formation of melt ponds is implicitly account for, since Shine and Henderson-Sellers' (1985) parametrisation assumes a pond areal fraction of 15% when the surface is melting. Morales Maqueda (1995) carried out an analysis of the model sensitivity to variations in the parameters included in the albedo formulation. This analysis showed that the simulated Arctic and Antarctic ice covers are far less responsive to albedo uncertainties than suggested by thermodynamic-only models.

The sea-ice model is coupled to an upper-ocean model, which consists of an integral mixed-layer model coupled to a diffusive model of the pycnocline. Advection of heat and salt by oceanic currents and run-off forcing are implicitly accounted for by restoring the temperatures and salinities of the water column to observations.

At the surface, the coupled model is driven by atmospheric fluxes determined from monthly climatological data fields by using bulk formulae (see FMM for details). In particular, snow deposition is derived from the monthly mean water-equivalent-precipitation rates of Jaeger (1976) by assuming that the fraction of precipitation falling as snow is a function of surface air temperature alone (Ledley 1985).

As mentioned already, the snow–sea-ice model used in the present work features a number of modifications with respect to FMM. These are described in the following paragraphs.

Owing to the large magnitude of the surface latent heat flux in the Southern Ocean (Andreas and Ackley 1982), mass losses due to sublimation of snow and ice are probably non-negligible there. (A comparison of the simulations discussed in Sect. 3.1 provides evidence of the potential importance of sublimation for the Antarctic ice pack.) In view of this fact, variations in snow and ice depths due to surface sublimation and condensation have now been incorporated into the model. Following Neeman et al. (1988), the rates of change of the snow and ice thicknesses resulting from these processes are

$$\left(\frac{\partial h_s}{\partial t}\right)_{subl} = \frac{F_{le}}{\rho_s(L_c + L_f)} \qquad h_s > 0; \quad h_s = 0 \text{ and } F_{le} > 0 \tag{1}$$

$$\left(\frac{\partial h_i}{\partial t}\right)_{subl} = \frac{F_{le}}{\rho_i(L_c + L_f)} \qquad h_s = 0 \text{ and } F_{le} \leq 0 \tag{2}$$

where h_s and h_i are the thicknesses of snow and ice, respectively, t is time, ρ_s ($=330\,\mathrm{kg\,m^{-3}}$) and ρ_i ($=900\,\mathrm{kg\,m^{-3}}$) are the densities of snow and ice, respectively, L_c ($=2.5\times10^6\,\mathrm{J\,kg^{-1}}$) is the snow/ice

latent heat of vaporization, L_f ($=0.334 \times 10^6$ J kg^{-1}) is the snow/ice latent heat of fusion, and F_{le} is the turbulent flux of latent heat. Hoarfrost formation by condensation is treated as snow deposition.

The parametrisation of snow-ice formation has also been revised. Of the mechanisms of snow-ice production listed in Sect. 1, only the one related to the isostatic equilibrium of the ice cover is represented in our model. Snow-ice formation is initiated whenever the imbalance

$$h_d = \frac{\rho_s h_s + \rho_i h_i}{\rho_w} > h_i \tag{3}$$

occurs, where h_d is the ice draft and ρ_w ($=1024.458$ kg m^{-3}) is the reference density of seawater. At this stage, seawater infiltrates the submerged snow, which increases in density due to the settling of snow grains (Eicken et al. 1995). The seawater–snow mixture transforms into snow ice and the new isostatic equilibrium is given by

$$\rho_s(h_s - (\Delta h_s)_{si}) + \rho_i(h_i + (\Delta h_i)_{si}) = \rho_w(h_i + (\Delta h_i)_{si}) \tag{4}$$

$$(\Delta h_s)_{si} = \beta_{si}(\Delta h_i)_{si} \tag{5}$$

where h_s and h_i are the snow and ice thicknesses prior to the formation of snow ice, respectively, $-(\Delta h_s)_{si}$ is the change in snow thickness, $(\Delta h_i)_{si}$ is the change in ice thickness, and β_{si} is an empirical parameter taking into account the compaction mentioned of the soaked snow. The total mass of newly formed snow ice, $\rho_i(\Delta h_i)_{si}$, consists of a meteoric ice contribution from the wetted snow, $\rho_s(\Delta h_s)_{si}$, and a contribution from the infiltrated seawater, $(\rho_i - \beta_{si}\rho_s)(\Delta h_i)_{si}$. The fractional contribution of snow to the total mass of snow ice is taken constant. On the basis of observations of west Antarctic ice floes by Jeffries et al. (1994a) in which the fraction of meteoric ice in snow ice was $41.2 \pm 24.0\%$, we have deduced a value for β_{si} of 1.1236. (This figure will have to be revised since it appears that the meteoric ice fraction reported by Jeffries et al. 1994a overestimates the contribution of snow to snow ice by a factor of around 2; see Jeffries et al. 1997.) Eicken et al. (1995) use $\beta_{si} = 1.5$ as determined from field data in the Weddell Sea. However, the results of Lange et al. (1990) for the same region suggest that this figure might actually be rather smaller. Substituting $\beta_{si} = 1$ in Eq. (5) yields the parametrisation utilised in FMM. Setting β_{si} equal to ρ_i/ρ_s is equivalent to making the unrealistic assumption that no seawater penetrates the submerged snow matrix during an episode of snow-ice formation.

Natural conditions would be better represented in the model by treating snow ice as an independent ice layer. However, to keep the thermodynamic calculations simple, snow ice and black ice (the ice formed from the basin water alone) are not treated separately. Whenever snow-ice formation takes place, the layer of snow ice that has just been created is incorporated at the top of the pre-existing ice. The temperature of the newly formed snow ice, T_{si}, is determined as a weighted average of the snow layer and infiltrated water temperatures. T_{si} being known, a second weighted formula provides the new internal ice temperatures (the temperature of the overlaying snow remains unchanged). Notice that, according to this procedure, the upper ice layer tends to warm as a result of snow-ice formation. This warming causes a decrease in the conductive heat flux at the base of the ice cover, but at the same time, it stimulates heat conduction through the snow–ice interface. This phenomenon has actually been observed in sea ice in the western Weddell Sea (Lytle and Ackley 1996). For simplicity, we neglect the density difference between snow ice and black ice (typical densities for these two ice types are 880 and 910 kg m^{-3}, respectively; Leppäranta 1983).

Snow ice is a much poorer heat conductor than black ice and, as a rule, its presence markedly affects the vertical profile of the ice thermal conductivity. Faithfully representing this effect would require the introduction in the model of a depth-dependent thermal conductivity. To obviate this complication, an average thermal conductivity for the entire ice column, k_e, is derived by supposing a non-divergent conductive heat flux from the top to the bottom of the ice:

$$k_e = \left(1 + \left(\frac{k_i}{k_{si}} - 1\right)\frac{h_{si}}{h_i}\right)^{-1} k_i \tag{6}$$

where k_i ($=2.0344$ W m^{-1} K^{-1}) and k_{si} ($=0.5$ k$_i$, as in Leppäranta 1983) are respectively the thermal conductivities of seawater ice and snow ice, which for ease of the computations are taken constant, and h_{si} is the snow-ice thickness. The latent heat and the brine released in the freezing of the seawater component upon snow-ice formation are discharged into the mixed layer.

Our scheme for snow-ice formation is highly idealised and the choice of values for β_{si} and k_{si} lends itself to large uncertainties. We have performed a number of experiments to test the model sensitivity to changes in these parameters. We will not discuss the results of these experiments in detail. Nonetheless, it is worthwhile mentioning that the range of variation of the annual mean Antarctic snow-plus-ice mass is -0.1×10^3 km^3 of ice (-0.6% of the annual mean mass) for β_{si} varying between 1.1236 and 2.7273 ($=\rho_i/\rho_s$). For values of k_{si} between 0.15 k$_i$ and k_i, the corresponding range of variation is $+0.7$ ($+4\%$ of the annual mean mass). The sensitivities of the total snow and ice masses are reassuringly small (although the relative change in snow-ice mass for varying β_{si} is, in fact, rather large). We conclude that uncertainties in β_{si} and k_{si} do not seriously affect the model behaviour, with the exception of its snow-ice component.

3 Sensitivity experiments

In FMM, two sensitivity experiments were conducted in order to assess the impact of snow and snow-ice formation on the characteristics of the Arctic and Antarctic ice packs. In the first experiment, snow was not allowed to accumulate on top of sea ice. In the second one, the parametrisation of snow-ice formation was not activated. It was found that, in the Northern Hemisphere, the absence of snow deposition on sea ice has little effect on the ice areal coverage and only a moderate enhancing effect on the total ice volume. In the Southern Hemisphere, neglecting the presence of snow led to a noticeable southward shift of the summer ice edge and to significantly different ice-thickness patterns in the western sector of the Southern Ocean. It was also found that the suppression of snow-ice formation is of no major consequence to the Arctic ice pack, while it crucially modifies the distributions of snow and ice thicknesses in the Weddell, Bellingshausen, Amundsen, and Ross Seas. The results obtained when these two experiments are repeated with the new version of the model are qualitatively the same as those in FMM and will not be discussed.

The experiments presented deal with the spatiotemporal changes in the distribution patterns of snow and sea ice due to variations in (1) the sublimation/condensation rate, (2) the precipitation rate, and (3) the amount of snowfall transported by the wind into leads. Table 1 summarises the experiments performed with the model. In each of them, the coupled snow–sea-ice–upper-ocean model was integrated for 10 y under prescribed atmospheric and oceanic forcings. By the end of the integration, the model reached in all the cases an

Table 1 List of experiments

Label	Description
1a	Sublimation (condensation) mass loss (gain) equal to 100% of net evaporative flux
1b	Sublimation (condensation) mass loss (gain) equal to 50% of net evaporative flux
1c	Sublimation (condensation) mass loss (gain) equal to 25% of net evaporative flux
1d	Sublimation (condensation) mass loss (gain) equal to 0% of net evaporative flux (CONTROL EXPERIMENT)
2a	Total precipitation reduced by 50%
2b	Total precipitation reduced by 25%
2c	Total precipitation increased by 25%
2d	Total precipitation increased by 50%
3a	Fraction of snowfall blown into leads equal to 25%
3b	Fraction of snowfall blown into leads equal to 50%

equilibrium seasonal cycle from which the results presented are issued.

For the analysis of the results, we have divided the Southern Ocean into five geographical sectors, namely, the Weddell Sea, the Bellingshausen–Amundsen Seas, the Ross Sea, the western Pacific Ocean sector, and the Indian Ocean sector. The geographical demarcation of these five areas is shown in Fig. 1. For each of these sectors, we have computed the total snow-plus-ice mass, M, the total snow mass, M_s, and the total snow-ice mass, M_{si}. Since the ice density takes a constant value in our model, M, M_s, and M_{si} can be expressed in terms of an equivalent ice volume, which we do. Tables 2, 3, and 4 assemble the sector-by-sector annual mean values of these variables for the various sets of experiments.

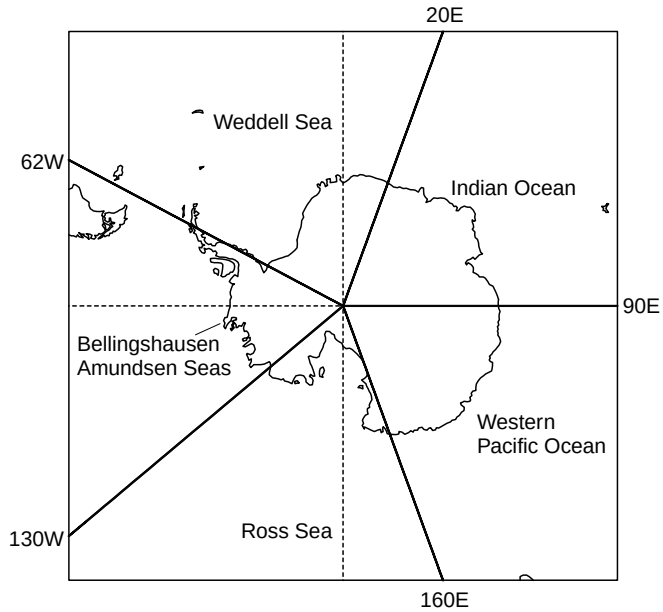

Fig. 1 Sectors of the Southern Ocean used for the analysis of the model results

3.1 Sublimation/condensation

In the following experiments, we attempt to estimate the contribution of the sublimation/condensation process to the mass budget of the snow–sea-ice cover. Latent heat fluxes over sea ice in the central Arctic are usually less than $5\ \mathrm{W\,m^{-2}}$ and directed towards the atmosphere (Barry et al. 1993). Typical annual mean values produced by our model are of the order of $4\ \mathrm{W\,m^{-2}}$. On the basis of these figures, the effect of

Table 2 Sector-by-sector contributions of snow and snow ice to the annual mean snow-plus-ice mass in the Southern Ocean for the experiments on sublimation/condensation

Experiment		Weddell Sea	Bellingshausen–Amundsen Seas	Ross Sea	Western Pacific Ocean	Indian Ocean	Southern Ocean
	M	5.6	3.4	4.4	1.0	1.6	16.1
1a	M_s/M	6.4	8.6	4.8	5.9	2.3	6.0
	M_{si}/M	1.3	16.9	0.3	10.3	0.1	4.7
	M	5.9	3.5	4.5	1.0	1.6	16.6
1b	M_s/M	8.7	9.0	6.6	6.8	4.4	7.7
	M_{si}/M	4.1	22.4	0.8	18.5	0.3	7.5
	M	6.1	3.6	4.5	1.1	1.7	16.9
1c	M_s/M	9.7	9.1	8.8	7.3	5.6	8.8
	M_{si}/M	7.4	24.2	3.7	19.8	0.5	10.1
	M	6.2	3.6	4.6	1.1	1.7	17.2
1d	M_s/M	10.2	9.2	9.3	7.8	6.7	9.2
	M_{si}/M	10.9	26.5	6.7	21.3	1.0	12.8

See Table 1 for the description of the experiments. M, M_s, and M_{si} are the snow-plus-ice mass, the snow mass, and the snow-ice mass, respectively. All three are in 1×10^3 km^3 of ice. The ratios M_s/M and M_{si}/M are given in per cent

Table 3 As in Table 2, except for the experiments on precipitation

Experiment		Weddell Sea	Bellingshausen–Amundsen Seas	Ross Sea	Western Pacific Ocean	Indian Ocean	Southern Ocean
	M	5.9	2.7	4.2	0.9	1.5	15.2
2a	M_s/M	6.9	6.8	5.9	4.5	3.4	6.1
	M_{si}/M	1.3	2.5	0.1	3.6	0.2	1.2
	M	6.0	3.1	4.4	0.9	1.6	16.1
2b	M_s/M	9.0	8.3	8.3	6.2	5.1	8.1
	M_{si}/M	5.1	12.3	1.4	6.8	0.5	5.2
	M	6.5	4.2	4.9	1.2	1.7	18.7
2c	M_s/M	10.8	9.7	9.7	8.6	7.9	9.8
	M_{si}/M	17.5	42.3	14.3	27.8	2.4	21.6
	M	7.0	5.1	5.3	1.4	1.8	20.6
2d	M_s/M	11.1	10.1	10.0	9.2	8.8	10.2
	M_{si}/M	24.8	55.6	21.6	33.8	4.9	30.4

Table 4 As in Table 2, except for the experiments on blowing snow

Experiment		Weddell Sea	Bellingshausen–Amundsen Seas	Ross Sea	Western Pacific Ocean	Indian Ocean	Southern Ocean
	M	6.3	3.2	4.6	1.0	1.7	16.7
3a	M_s/M	6.9	6.3	5.6	4.8	3.4	6.0
	M_{si}/M	1.1	1.8	0.1	6.4	0.2	1.2
	M	6.1	3.4	4.6	1.0	1.7	16.7
3b	M_s/M	9.0	8.2	8.2	6.3	5.1	8.1
	M_{si}/M	5.0	10.9	1.2	10.0	0.5	5.0

surface sublimation/condensation on the mass balance of the Arctic pack is anticipated to be small. By contrast, the lower moisture content and stronger winds imperating in the Antarctic are conducive to much larger latent heat losses. In our model, latent heat fluxes over sea ice in the Southern Ocean can be more than three times larger than those in the Arctic, with annual mean values around 15 $W m^{-2}$ (mid-spring measurements over the interior pack in the eastern Weddell Sea indicate values oscillating between 0 and 30 $W m^{-2}$; Andreas and Makshtas 1985). It has been observed, however, that these fluxes are transferred only a few metres above the surface and are relayed back to the ice downwind by, among other processes, water-vapour condensation and ice-crystal precipitation (Barry et al. 1993). Thus, the effective mass loss due to sublimation is likely to be sensibly smaller than implied by considering the surface latent heat flux alone. To account for these redeposition mechanisms, the rate of mass loss (gain) associated with sublimation (condensation) has been prescribed in the model to be a constant fraction γ_{subl} of the total surface sublimation/condensation flux. Four values of γ_{subl} were tested: 1, 0.5, 0.25, and 0.

Figure 2 depicts the seasonal variations of the total precipitation and snowfall in the Northern and Southern Hemispheres poleward of 60 °N and 60 °S, respectively, together with the total areas and volumes of snow, ice, and snow ice simulated by the model when $\gamma_{subl} = 1$ (experiment 1a). The modelled Arctic ice pack is entirely covered by snow during most of the boreal winter. Both the snow and ice edges begin their northward retreat by mid-March. However, the snow area decreases slightly faster than the ice area as a consequence of the relatively intense sublimation in the subarctic regions. In April, snow sublimation can account for local losses of more than 0.05 m of snow per month (comparable or slightly larger than the corresponding precipitation rates at that time) in the Baffin Bay, Greenland, Bering, and Okhotsk Seas (measurements over land in northern Russia have yield monthly sublimation rates during April of about 0.02 m per month; Male and Granger 1981). Surface melting at the ice edge commences the second week of May. At this stage, the snow depth averaged over the entire area covered by ice is close to 0.2 m. In June, the decay of the snow cover accelerates, leaving exposed wider and wider stretches of the pack. Snow has nearly disappeared from the Arctic by the end of that month. Deposition of snowfall does not re-start until mid-August. By the end of October, a thin snow cover (0.03 m, on average) overlays already most of the Arctic ice.

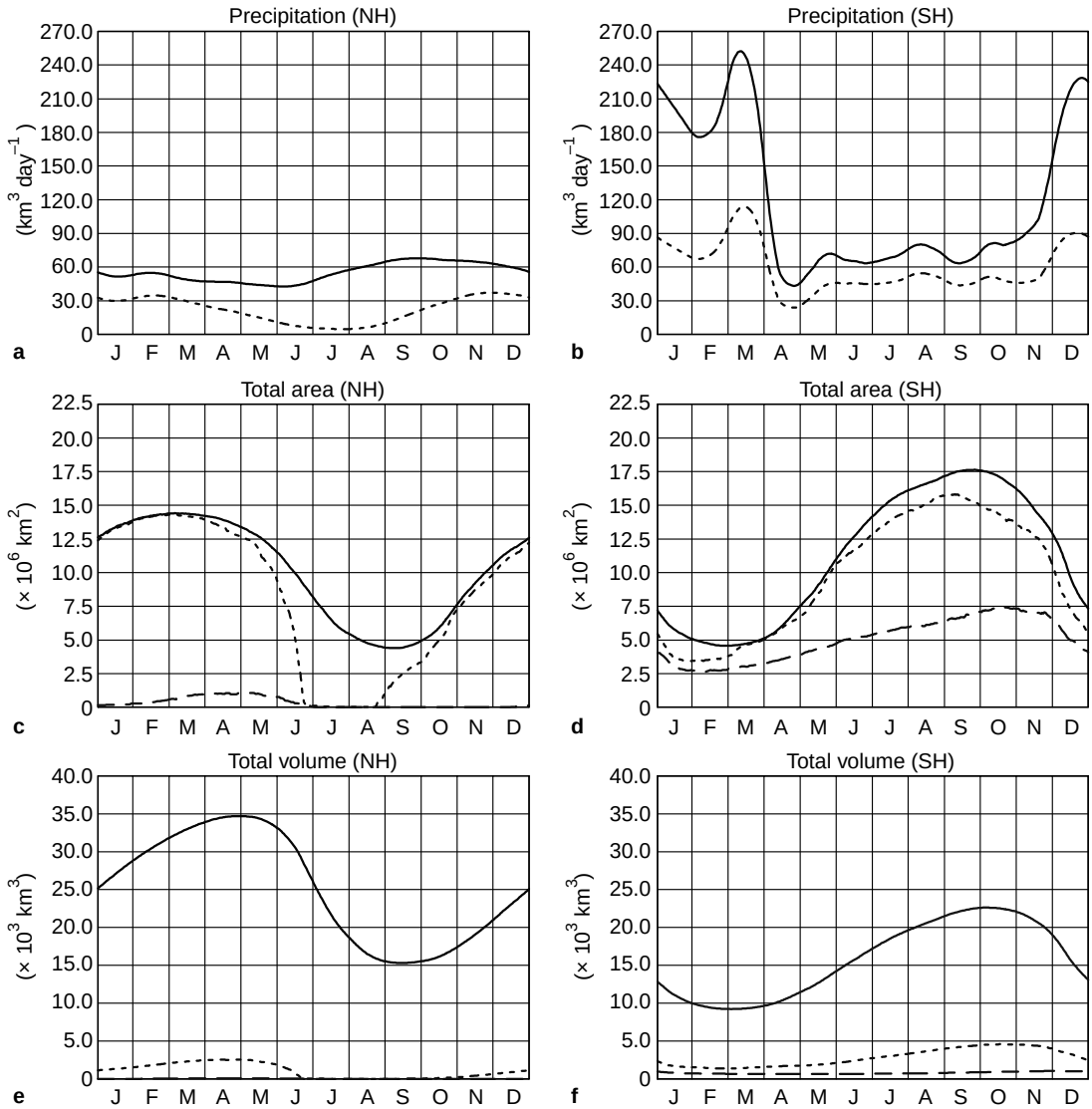

Fig. 2 a Seasonal cycles of Jaeger's (1976) total (liquid-plus-solid) precipitation (*solid*) and snowfall (*dashed*) over the oceanic area north of 60 °N (both are given in equivalent snow volume per day). **b** Same as **a**, except for the oceanic area south of 60 °S. **c** Seasonal cycles of the total snow (*short dashed*), ice (*solid*), and snow-ice (*long dashed*) areas in the Northern Hemisphere from experiment 1a. **d** Same as **c**, except for the Southern Hemisphere. **e** Seasonal cycles of the total snow (*short dashed*), ice (*solid*), and snow-ice (*long dashed*) volumes in the Northern Hemisphere from experiment 1a. **f** Same as **e**, except for the Southern Hemisphere

A very small amount of snow ice is produced during late winter and the first half of spring. This snow-ice formation, which contributes up to 0.2 m to the local ice growth, occurs mostly in a limited area situated to the east of Svalbard, where ice is never thicker than 1–1.5 m and where high precipitation rates during winter generate an accumulation of up to 0.6–0.8 m of snow by the end of April. We are not aware, unfortunately, of any field study on snow-ice formation in this region against which to contrast this finding.

The simulated seasonal cycles of the snow and snow-ice covers in the Southern Hemisphere are significantly different from those in the Northern Hemisphere. The area occupied by snow is sensibly smaller than the sea-ice area virtually all year long. In early spring, up to 15% of the ice pack is free of snow. This snow-free ice is mainly located in the marginal ice zones of the eastern Ross Sea and of the western Pacific and Indian sectors of the Southern Ocean (Fig. 3). Spring observations in the Indian Ocean sector indicate that more than 10% of the ice coverage in this region can be free of snow (Allison et al. 1993). Snow fully covers the winter ice in the Weddell Sea and in the Bellingshausen–Amundsen Seas, whereas data collected in this area during August–September 1993 (Worby et al. 1996) show that bare ice accounts for up to 14% of the ice areal coverage in this sector. The snow cover reaches its maximum volume between October and November, the average

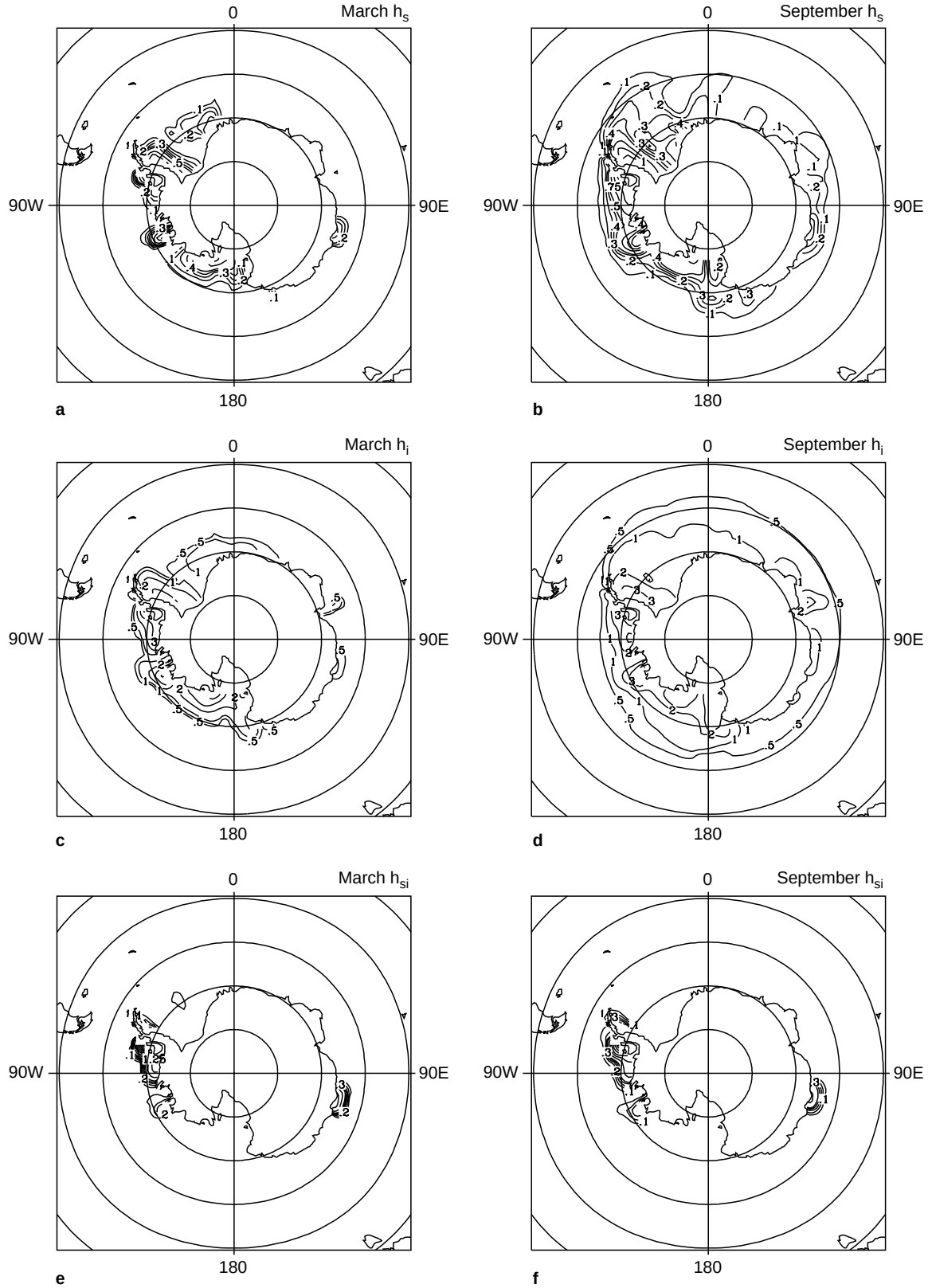

Fig. 3a–f Monthly fields of snow, ice, and snow ice thicknesses in the Southern Hemisphere from experiment 1a. **a** March snow thickness, **b** September snow thickness, **c** March ice thickness, **d** September ice thickness, **e** March snow-ice thickness, and **f** September snow-ice thickness. The contour interval for snow and snow-ice thicknesses is 0.1 m for values below 0.5 m and 0.25 m for values above 0.5 m. The contour interval for ice thickness is 0.5 m for values below 1 m and 1 m for values above 1 m

snow depth being around 0.3 m at that time. It follows a relatively rapid decay of the snow cover that ends by mid-February, at which moment a fraction of about 40% of the pack is free of snow. Note that during December and January, the difference between the total ice and snow areas, i.e. the area occupied by bare ice, remains almost constant or gently increases. The snow-free ice is certainly melting during this period, and therefore, the only mode whereby its area can be prevented from shrinking is the simultaneous removal of snow over snow-covered ice. Since neither lateral melting nor snow-ice formation can generate a decrease of snow fraction in the model, one must conclude that steady surface melting and/or sublimation are at work over parts of the interior pack. This will be discussed later in this section.

Snow-ice production is far more vigorous in the Antarctic than it is in the Arctic. Snow ice can occupy a large area during austral spring. However, most of this snow ice is seasonal and less than 0.1 m thick. Perennial snow ice contributes more than 70% to the total snow-ice volume in any season, but it covers a very modest area (Fig. 2d–f). The maximum in snow-ice volume arises shortly after the maximum in snow volume, by the end of November. The average snow-ice thickness is then close to 0.17 m, to be compared with a corresponding average ice thickness of 1.4 m. Figure 3 and Table 2 show that most of the snow ice is encountered in the Weddell, Bellingshausen, and Amundsen Seas and in the western Pacific sector of the Southern Ocean. The percentage of snow ice in sea ice predicted by the model in the Weddell Sea appears much smaller than the few observational estimates available. Analyses by Lange et al. (1990) and Eicken et al. (1994) suggest that the contribution of meteoric ice to the total ice mass, f_m, in the Weddell Sea during winter could range between $3 \pm 3\%$ and $3.6 \pm 5.4\%$, although there is a strong regional contrast in f_m between the western and central/eastern Weddell Sea. Bearing in mind that, in our parametrisation, the ratio of meteoric ice mass to snow-ice mass is constant (41%), one can deduce from Table 2 that the simulated amount of meteoric ice counts for a far too small 0.6% of the total Weddell Sea ice mass. By contrast, in the Bellingshausen–Amundsen Seas sector, the model estimate of f_m (7.6%), although probably somewhat large, falls close to the range of current uncertainty (2.4 to 5.6%; Jeffries et al. 1994a). The overall contribution of snow ice to the annual mean total ice volume in the model amounts to 5% (8% for multiyear ice). This is a somewhat puzzling result because in FMM this figure was as high as 15% (20% for multiyear ice). The comparison with the model response in the subsequent experiments will allow us to understand this behaviour.

Steadily diminishing the value of γ_{subl} yields, in both hemispheres, an increase in the snow accumulation rate and, consequently, an increase in the area and volume of the snow cover. During winter months, the snow cover becomes thicker and, because of the stronger thermal insulation, the ice cover thins slightly. Both effects conspire to enhance the formation of snow ice. In the Arctic, the summer response to the reduced sublimation rates is virtually nil, simply because the turbulent heat fluxes are by far overridden by the radiative ones and the snow cover totally melts away. In the Antarctic, the response of the summer ice pack is dictated by the enhanced snow areal coverage, which shields large portions of the ice cover against the incoming solar radiation, and by the intensified snow-ice formation during spring, which partly compensates for the subsequent summer ice melt. The result is a mild increase in both ice area and volume. We will comment here on the results from the experiment with $\gamma_{subl} = 0$ (experiment 1d).

Figure 4 displays the seasonal cycles of the total areas and volumes of snow, ice, and snow ice in both hemispheres for experiment 1d. In the Northern Hemisphere, the total ice area and volume are hardly affected by the suppression of the sublimation/condensation process, although the winter ice cover is, on average, 0.05 m thinner than in experiment 1a. The snow area behaves much the same as in experiment 1a throughout winter, but in the absence of surface sublimation, the snow remains thick enough during April to still cover the entire ice pack. As in experiment 1a, surface ablation begins by mid-May, when the average snow depth is at a peak of 0.25 m, and the melting of the snow cover is completed by the end of June. The snow cover does not reappear before the middle of August. In contrast to experiment 1a, in which sublimation noticeably delayed the autumn advance of the snow cover, a snow cap (0.007 m thick, on average) already covers the whole ice pack by early September. The area of snow ice formed eastward of Svalbard nearly doubles with respect to experiment 1a, but the amount of ice produced by this process remains relatively low.

In the Southern Hemisphere, the differences between experiments 1a and 1d are more prominent. The total ice area is roughly the same for both experiments throughout fall, winter, and spring, but during summer, sea ice covers up to 0.5×10^6 km^2 more oceanic area than in experiment 1a. The largest differences in ice volume between the two experiments are of the order of 0.5×10^3 km^3. By the end of the ice growth season, the total ice volume in experiment 1d is slightly smaller than in experiment 1a as a consequence of the enhanced thermal insulation. Conversely, by the end of the ablation season, it has become somewhat larger due to the accentuation of the snow–albedo effect and the strengthening of snow-ice formation. The snow and sea-ice areas essentially coincide during most of the seasonal cycle (see also Fig. 5), which demonstrates that the winter and spring bare ice encountered in experiment 1a is the result of snow losses by sublimation. In average over the entire Antarctic ice pack, the mass loss induced by surface sublimation in experiment 1a varies

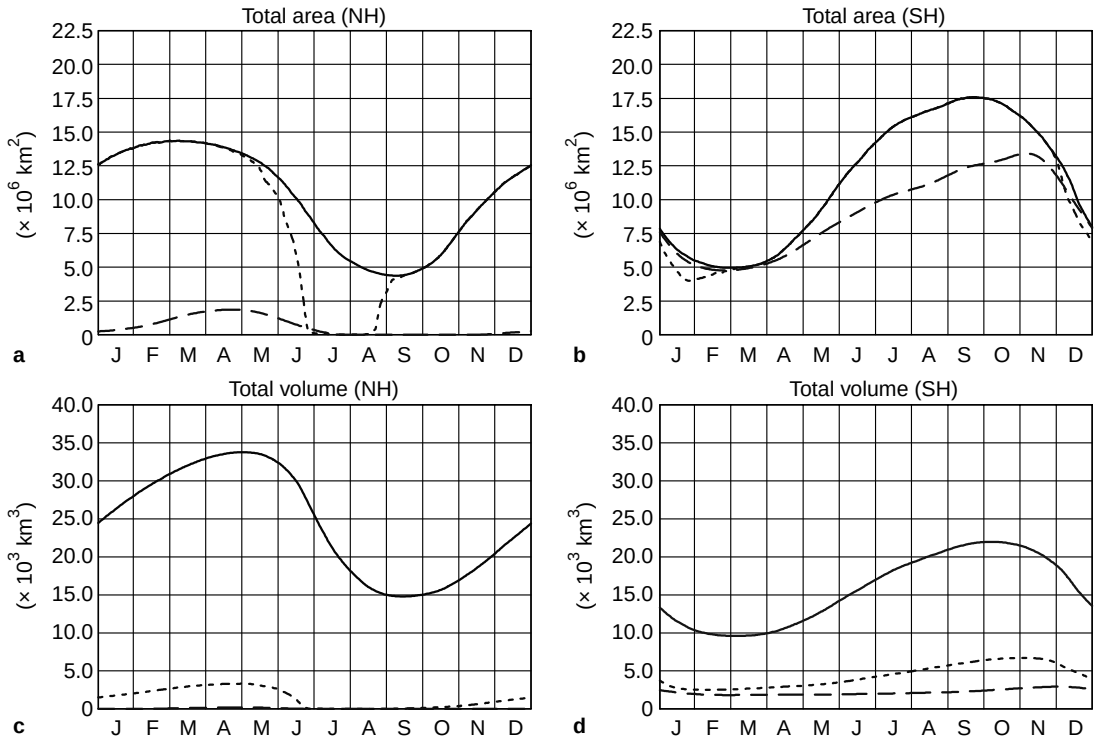

Fig. 4 **a** Seasonal cycles of the total snow (*short dashed*), ice (*solid*), and snow-ice (*long dashed*) areas in the Northern Hemisphere from experiment 1d. **b** Same as **a**, except for the Southern Hemisphere. **c** Seasonal cycles of the total snow (*short dashed*), ice (*solid*), and snow-ice (*long dashed*) volumes in the Northern Hemisphere from experiment 1d. **d** Same as **c**, except for the Southern Hemisphere

from 0.02 m of snow per month at the height of the winter season to 0.07 m per month by mid-summer. As is apparent from Table 2 and cross-inspection of Figs. 3a, b and 5a, b, the bulk of these evaporative losses takes place in the Weddell and Ross Seas and in the Indian Ocean sector. In these regions, local differences in snow thickness between experiments 1d and 1a can be as high as 0.6 m. In experiment 1d, only from December to February some regions of the ice edge, representing no more than 30% of the total ice area, are free of snow as a result of surface melting. When the snow cover reaches its maximum volume by mid-November (two weeks later than in experiment 1a), the average snow thickness is 0.44 m, i.e. more than 25% larger than in experiment 1a. The snow-mass increase in this simulation leads to a concomitant enhancement of snow-ice production. Between November and April, the snow-ice area is 85% or more of the total ice area. When the snow-ice sheet reaches its maximum volume by the end of November, its average thickness is 0.25 m, against 1.4 m for the average ice thickness. Figure 5 and Table 2 reveal that the amount of snow ice in the Weddell Sea experiences an eightfold increase, f_m becoming equal to 4.9%, a value which is much closer to observations. The fractions of snow ice in the Bellingshausen–Amundsen Seas and in the western Pacific Ocean sector increase by more modest amounts, and sea ice in the Ross Sea includes now a significant volume of snow ice (early winter observations of snow and ice in the Ross Sea, presented by Jeffries and Adolphs 1997, indicate that snow-ice formation is very active in this region).

We have seen that, in our model, surface sublimation has a considerable effect on snow-cover conditions in the Southern Ocean and, collaterally, on snow-ice formation. However, since little is known from either observational or modelling studies on snow and ice evaporative processes in polar regions, it is difficult to weigh the validity of this result, particularly when considering that a fraction of the sublimation products is likely to return back to the surface after condensation in the atmosphere. In experiment 1a, sublimation is responsible for the removal of 0.45 m of snow per year, on average, over the Antarctic ice pack. This yields simulated snow-thickness patterns that are generally in better agreement with observations than those from experiment 1d, although in both cases, the model tends to somewhat overestimate the snow thickness (see Allison et al. 1993; Eicken et al. 1994; Jacka et al. 1987; Jeffries et al. 1994a, b; Lange and Eicken 1991; Lange et al. 1990; Massom et al. 1997; Wadhams et al. 1987; Worby et al. 1996; Jeffries and Adolphs 1997). On the other hand, experiment 1a generates a seemingly very small amount of snow ice in the Weddell Sea, one of the few sites where observations of this phenomenon are available. Since one of the purposes of our investigation

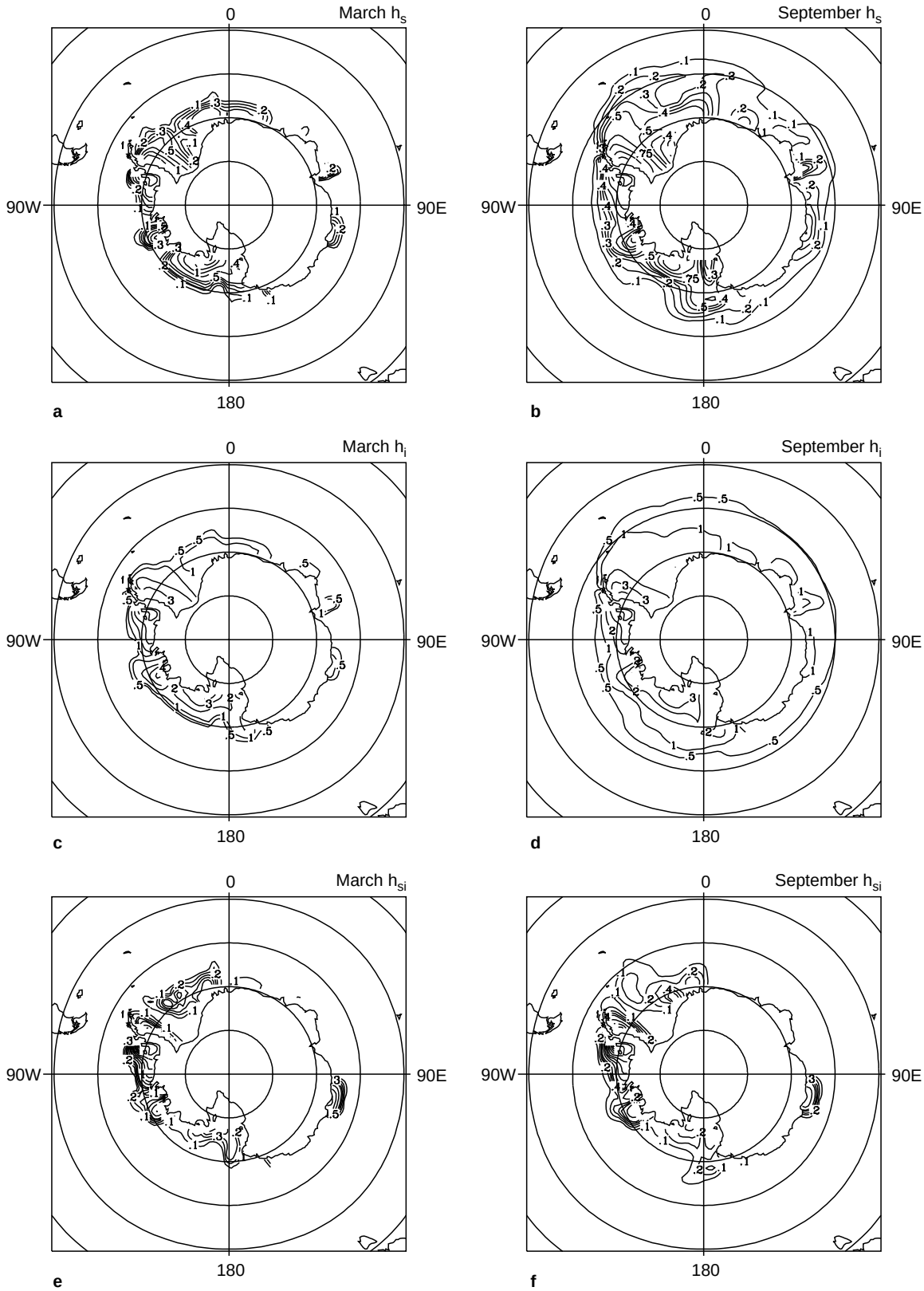

Fig. 5a–f As in Fig. 3, except for experiment 1d

is to determine the sensitivity of snow ice to changes in snow accumulation and given the uncertainty as regards the effective influence of surface sublimation/condensation on the snow cover, we have decided to use experiment 1d, rather than 1a, as the control case for comparison in our subsequent experiments, which, accordingly, were carried out with $\gamma_{subl} = 0$.

3.2 Precipitation

In experiments 2a to 2d, the precipitation rate, P, was uniformly perturbed by percentages of -50%, -25%, $+25\%$, and $+50\%$, respectively. Reducing the precipitation rate in a model with $\gamma_{subl} = 0$ can be expected to have an impact similar to that of increasing the value of γ_{subl}. For example, our experiments reveal that snow, ice, and snow-ice changes in the Southern Ocean due to a reduction of 25% in P are of the same sign and quantitatively close to those produced by increasing γ_{subl} from 0 to 1 (compare experiments 1a and 2b in Tables 2 and 3, respectively). However, P is in our model an external parameter, whereas the sublimation/condensation rate is not. It is determined as a function of the surface latent heat flux, which in turn is diagnosed by the model in terms of the surface temperature. Uniformly modifying γ_{subl} will not therefore lead to a uniform perturbation in the sublimation/condensation rate. Varying the rate of precipitation is expected to impinge on the behaviour of the sea-ice cover via two chief mechanisms. First, variations in snow deposition will affect ice growth and decay by modifying heat conduction through ice, altering surface albedo and latent heat content (mass effect of snow), and changing the rate of snow-ice formation. Second, readjustments in upper-ocean stratification due to changes in the surface freshwater flux will affect the oceanic sensible heat flux to the ice and hence basal ice accretion and ablation. Owing to the strong constraint imposed by the relaxation towards observed annual mean salinities in the model, our simulations are unfortunately not the most adequate to gauge the actual impact of this second effect. Nevertheless, variations in precipitation do induce measurable shifts in the simulated mixed-layer salinities and oceanic heat fluxes that have a noticeable influence on the behaviour of the sea-ice cover.

Perturbing the precipitation rate has a relatively minor effect on the seasonal cycle of the Arctic sea-ice cover. Neither the snow nor the ice areas change by more than 2% with respect to those displayed in Fig. 4a. By contrast, the snow-ice area varies substantially with varying precipitation. It practically reduces to zero in experiment 2a and nearly doubles in experiment 2d. Yet, the mass of snow ice remains well below 2% of the total snow-plus-ice mass, even for a 50% increase in precipitation (although snow ice around Svalbard can grow to up a thickness of 0.4 m). Since snow-ice formation is very rare in the Arctic, most of the snow simply piles up on top of sea ice, and thus, fractional variations in snow volume essentially coincide in magnitude with the corresponding perturbations in the precipitation rate. As snow accumulation increases from experiment 2a to experiment 2d, the surface temperature of the snow cover slightly decreases. As a consequence of this cooling, the onset of snow ablation in May and the final disappearance of the snow cover by late June are gradually delayed, although by no more than five days in all. During winter and spring, the total ice volume undergoes a slight increase (decrease) for precipitation rates smaller (larger) than the control ones. This is due to the stimulation (inhibition) of heat conduction through ice which results from the thinning (thickening) of the snow cover. The increase (decrease) of the oceanic heat flux that follows from the modification of the surface freshwater input is never larger than $2\ \mathrm{W\,m^{-2}}$, on average, and is not enough to counterbalance the change in heat conduction. During summer, once snow has melted away, the ice volume becomes virtually the same in all the experiments. This insensitivity was to be expected because (1) the snow cover disappears all the same from the Arctic for approximately two months between late June and late August and (2) Jaeger's (1986) precipitation has a minimum over the central Arctic during this period. These results are at odds with those of Weatherly and Walsh (1996). Using a model of the coupled Arctic ice-ocean system with no artificial restoring to climatological salinities, these authors obtained a strong response of the ice cover to a suppression of precipitation. Contrary to our simulations, the ice thickness rapidly decreased in reaction to greater oceanic heat fluxes. Doubled precipitation resulted in a smaller increase in ice thickness. Although their unconstrained experiments are, in principle, more realistic than ours, it should be stressed that these authors significantly underestimated the surface salinity in their control run. This might be responsible to a certain degree for the enhanced sensitivity of sea ice in their model.

Figure 6 shows that the response of the Antarctic sea-ice cover in experiments 2a–d is more complex and stronger than that of the Arctic pack. The snow, sea-ice, and snow-ice covers exhibit all three sensitivities of the same sign to perturbations in precipitation. The snow and ice areas vary almost linearly with variations in the precipitation rate.

The changes in snow and ice volumes are less symmetrical. The maximum differences in snow volume between experiments 2a to 2d and experiment 1d occur in November, circa the maximum in snow volume. At this moment, the decrease in the average snow thickness is as large as 0.17 m (i.e. 40%) in experiment 2a, while the corresponding increase for experiment 2d is of only 0.06 m (i.e. 15%). In contrast with the response found in the Northern Hemisphere, the change in the

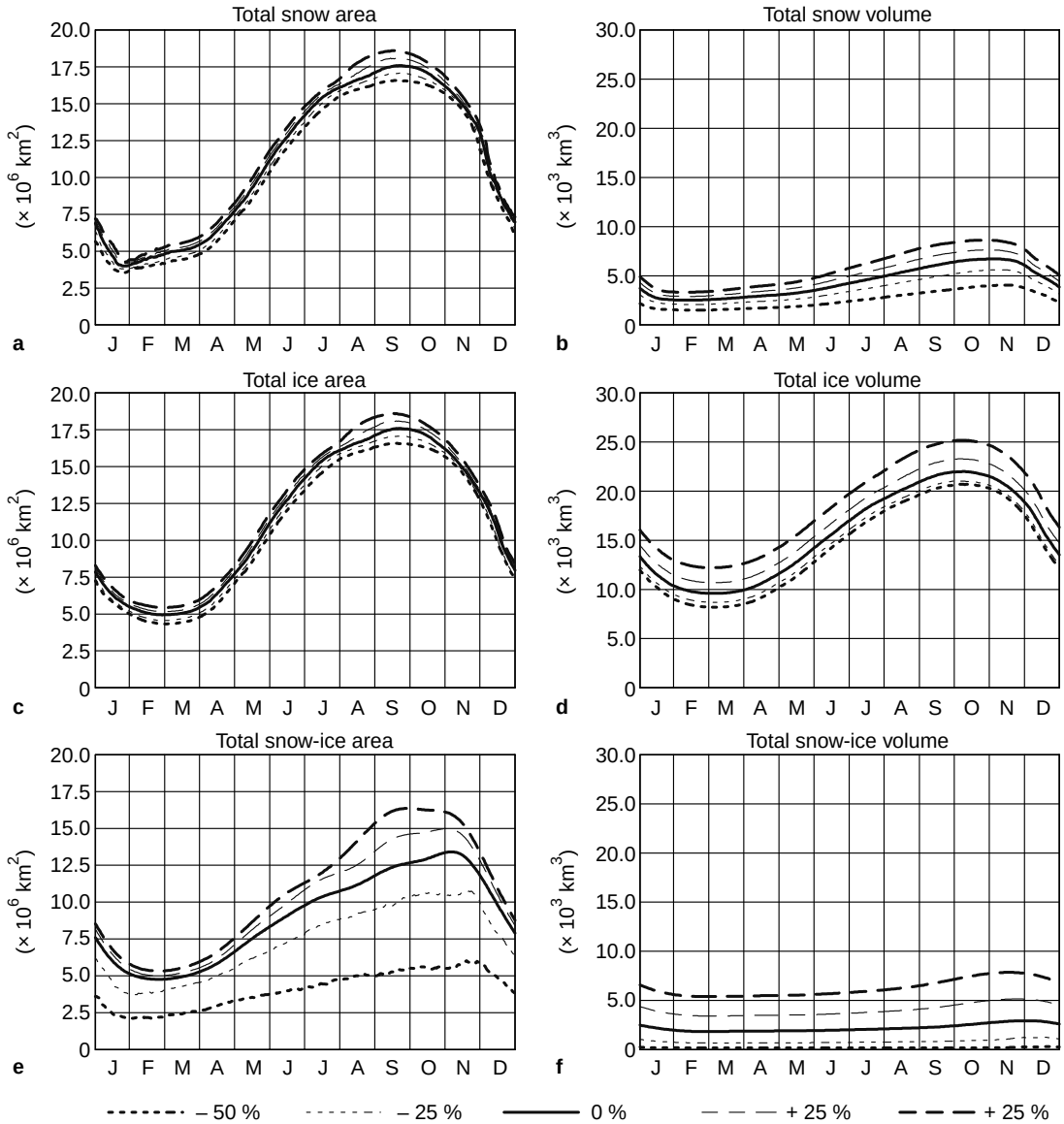

Fig. 6a–f Seasonal cycles of the total **a** snow area , **b** snow volume, **c** ice area, **d** ice volume, **e** snow-ice area, and **f** snow-ice volume in the Southern Hemisphere from experiments 2a, 2b, 1d, 2c, and 2d

amplitude of the seasonal cycle of the snow volume is not proportional, in general, to the change in snowfall rate, especially for the case of a large increase in precipitation. This is because of the buffering effect that snow-ice formation has on the net snow accumulation. If, for instance, precipitation increases, the rate of snow-ice production also increases (see Fig. 6f), thus restraining the accompanying increase in accumulation. The changes in ice volume are also strongly nonlinear, showing a much larger sensitivity for increasing precipitation rates than for decreasing ones. The annual mean ice thickness averaged over the whole pack, which equals 1.4 m in experiment 1d, diminishes (augments) by 5% (20%) in experiment 2a (2d). The magnitude of the response does not change much, however, from season to season.

Interestingly, the volume response in our simulations is exactly the reverse of that found by Eicken et al. (1995) with a large-scale snow–sea-ice–upper-ocean model. In their experiments, a decrease (increase) in the rate of snowfall was followed by an increase (decrease) in total ice volume. Clearly, the enhanced (reduced) shortwave radiation absorbed at the surface and the weaker (stronger) snow-ice formation were insufficient in their case to compensate for the reduced (enhanced) thermal insulation effect (the authors pointed out that the oceanic heat flux was not significantly affected by the changes in snowfall rate). There are several differences between the model of Eicken at al. (1995) and ours which preclude a detailed comparison of results. Furthermore, their simulations were 1-y-long transient runs, with a spatially and temporally uniform snowfall

rate, and were restricted to the Weddell Sea. In our study, the persistence of snow over most of the summer pack allows us to cast aside any major disparity in the behaviour of surface albedo and latent heat content between experiments. The model response to changes in precipitation is therefore basically determined by the competition between the thermal insulation effect of snow, the snow-ice formation, and the modification of the upper-ocean stratification caused by alterations in the oceanic haline forcing.

Although smaller precipitation rates lead to an enhanced heat conduction through ice, they do not bring about a net increase in the ice-growth rate, as it was the case in the work by Eicken et al. (1995). The reason for this is twofold. In the first place, the decrease in snow accumulation is very detrimental for snow-ice formation, as can be seen from Fig. 6f and Table 3. (In simulations 2a and 2b, the reduction in snow-ice volume is actually larger than the reduction in total ice volume.) In the second place, the decrease in the freshwater flux to the ocean yields higher mixed-layer salinities (the annual mean mixed-layer salinity under the ice pack increases by almost 0.2 psu between experiments 2a and 1d), which stimulates vertical mixing and yields a stronger sensible heat flux at the base of the ice (by mid-winter, the oceanic heat flux averaged over the entire ice pack is approximately $6\,W\,m^{-2}$ larger in experiment 2a than in experiment 1d). These two mechanisms tend to limit the top and bottom growths of ice, respectively, so as to slightly outbalance the effects of the enhanced heat conduction. The result is a decrease in ice production rate of about 0.02 m per month during fall and early winter. The converse behaviour is observed for precipitation rates larger than the control ones. However, the oceanic heat flux during the growth season is modified by more modest amounts than before. The salinity decrease in experiments 2c and 2d is of about the same size as the increase obtained in experiments 2b and 2a, respectively, but the resulting weakening of the winter oceanic heat flux is less than $3\,W\,m^{-2}$, on average. Note that the variations in snow-ice volume are in all experiments greater than the corresponding variations in total ice volume, which suggests that snow-ice formation is the process that prevails in controlling the ultimate response of the ice pack. Given the smallness of the changes of the oceanic heat flux in experiments 2c and 2d, we conclude that, in these experiments, the reinforced snow-ice formation is the factor chiefly responsible for the increased total ice volumes. This, in fact, is in agreement with the finding of Eicken et al. (1995) that accumulation rates larger than 1.5 m of snow per year (i.e. about twice the best observational estimate for the Weddell Sea to date) induce an increase in ice volume due to the growing contribution of snow ice. In experiments 2a and 2b, the role that the modifications of the upper-ocean stratification play in shaping the ice-volume response is somewhat more important (this will be confirmed in Sect. 3.3), although again it is the relative contributions of the variations in the bottom accretion rate due to the reduced thermal insulation and those in the top growth rate due to the weakened snow-ice formation that mainly dictates the equilibrium seasonal cycle of ice volume.

A last remark concerns the geographical distribution of the thickness response. Figure 7 and Table 3 indicate that, as in the experiments on sublimation/condensation, there is a marked east–west asymmetry in the sensitivity of the Antarctic ice pack. Variations in snow, ice, and snow-ice thicknesses are much larger in the western Southern Ocean, where snow and ice are thicker, than in the eastern Southern Ocean. The strongest sensitivity is observed in the Bellingshausen–Amundsen Seas sector, where the annual mean precipitation rates more than double those in the Weddell and Ross Seas. Interestingly enough, the ice thickness sligthly increases (decreases) in the southwestern Weddell Sea sector with decreasing (increasing) precipitation (see Fig. 7c, d). There, it is clearly the thermal insulation effect of snow that overrides all other effects (the amount of snow ice generated by the model is actually rather low in this area).

3.3 Blowing snow

Using empirical equations that relate the mass flux and mass concentration of drifting snow to the surface wind, Eicken et al. (1994) derived a conservative estimate for the loss of snow to leads by the blowing snow process. According to their calculations, the annual transfer of drifting snow to the ocean in the Weddell Sea could be of roughly 0.1 m of snow, which amounts to about 12% of the estimated snow accumulation. Thus, the transport of snow by the wind could significantly affect the net accumulation of snow on sea ice and the freshwater balance of the oceanic mixed layer. The introduction of a detailed a parametrisation of the snow-drift flux in the model (e.g. Mellor and Fellers 1986) would require precise information regarding surface winds, and therefore, could not be applied with the geostrophic wind forcing used in our model. In addition, estimating snow losses to leads as a result of wind transport would also require some hazardous assumptions about the average subgrid spacing between leads, of which very little is known. Instead, we have tried a much simpler, qualitative approach, whereby a spatially and temporally constant fraction γ_{blow} of the snowfall is prevented from accumulating on the ice and is immediately transferred to the ocean. For γ_{blow} between 0 and 20%, only minor changes were detected in the equilibrium total snow and ice areas and volumes. We found it instructive, however, to conduct experiments with relatively large values of γ_{blow}, namely, 25% and 50% (experiments 3a and 3b, respectively), in order to compare the model response with

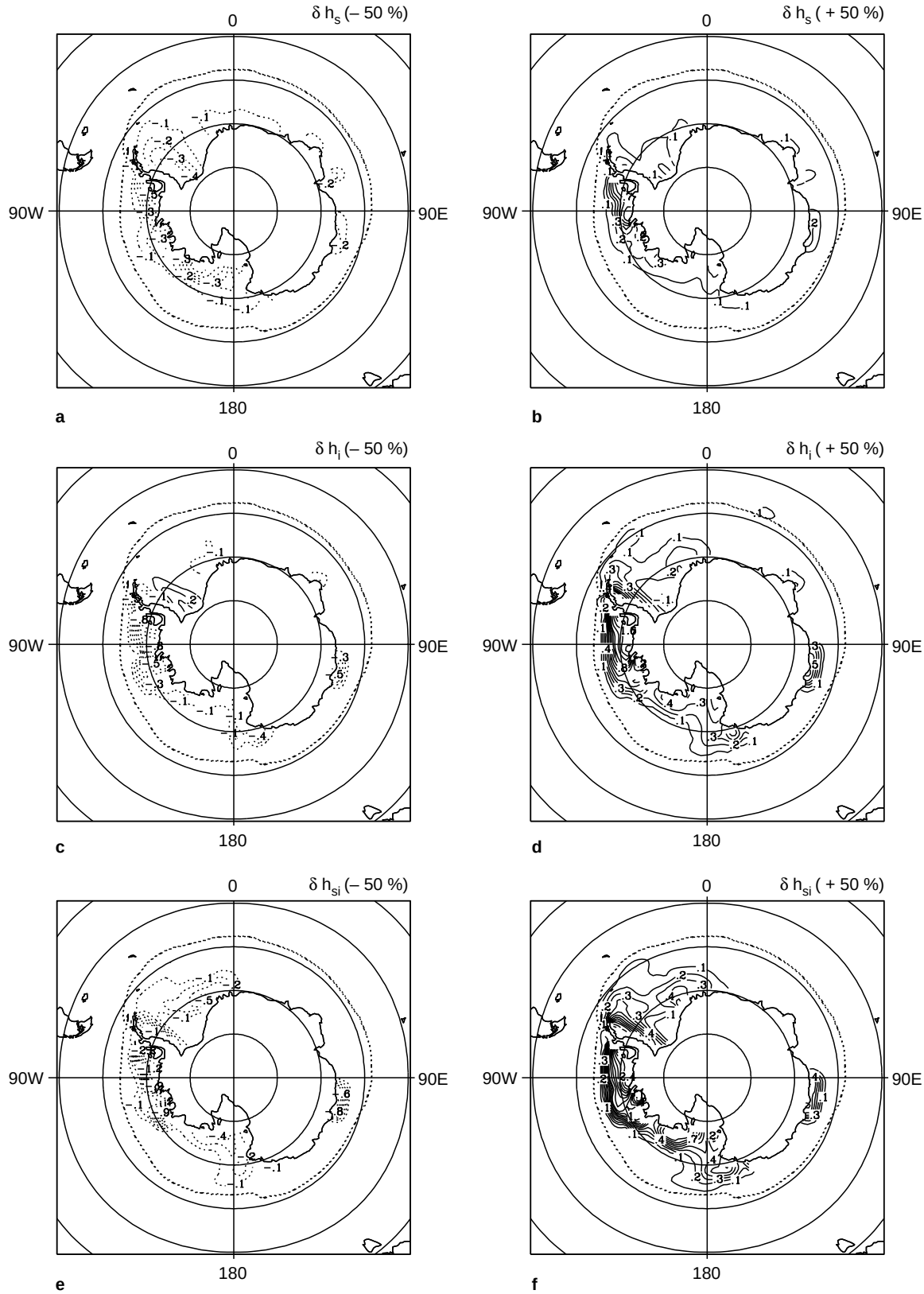

Fig. 7 **a** Distribution of the difference in annual mean snow thickness between experiments 2a and 1d over the Southern Ocean. **b** Distribution of the difference in annual mean snow thickness between experiments 2d and 1d over the Southern Ocean. **c** Same as **a**, except for ice thickness. **d** Same as **b**, except for ice thickness. **e** Same as **a**, except for snow-ice thickness. **f** Same as **b**, except for snow-ice thickness. The contour interval is 0.1 m for values between −1 and 1 m and 0.2 m otherwise. The *thick*, *stippled line* represents the 0.1 m ice-thickness contour from experiment 1d

that obtained in the previous section. The only actual difference between the two kinds of experiments is as regards the total freshwater input into the system, which has the potential to modify the upper-ocean stratification and hence the oceanic sensible heat flux to the ice. In experiments 2a–b, the total input of freshwater was reduced, while in the present experiments, it is the same as in the control case. We simply distribute it differently between the ice-covered and ice-free portions of the grid cells.

The results obtained both in the Northern and Southern Hemispheres are very similar to those from experiments 2a and 2b. The total snow and ice areas simulated by the model in the Southern Ocean (not shown) are virtually indistinguishable from those of experiment 1d. The same can be said about the total ice volume, although for experiment 3a, a very small increase during winter (due to the enhanced heat conduction) and an also small summer decrease (due to reduced snow-ice formation) occur. This contrasts with the results from experiments 2a–b, which show smaller ice volumes than in the control experiment throughout the year. As announced in Sect. 3.2, this different behaviour is explained by disparities in the upper-ocean stratification between the two sets of experiments. In experiments 3a and 3b, the net salt fluxes into the mixed layer change but little with respect to those in experiment 1d, and the differences in the average oceanic heat flux never exceed $+1.5\ \mathrm{W\,m^{-2}}$. The decreases in snow volume and in snow-ice area and volume are very close to those encountered in experiments 2a–b. Regarding the geographical distribution of the mass changes, it is helpful to compare Tables 4, 3, and 2 for experiments 3a, 2a, and 1d, respectively. Whereas a decrease of 50% in precipitation (experiment 2a) yields losses of snow-plus-ice mass in all Antarctic sectors, a decrease of the same magnitude in snow accumulation (experiment 3a) is conducive to much more modest losses or even slight gains, as in the Weddell Sea. The total ice mass increases, in fact, by a few percent in the Weddell and Ross Seas.

4 Summary and conclusions

We have performed a series of sensitivity experiments with a large-scale snow–sea-ice–upper-ocean model in order to quantify the influence of snow accumulation and snow-ice formation on the seasonal behaviour of the sea-ice cover. This investigation was motivated by numerical results reported by Eicken et al. (1995) and by Weatherly and Walsh (1996), which suggest that the Weddell Sea and Arctic sea-ice covers might be very sensitive to changes in precipitation. We have analysed the model response to variations in the surface evaporative flux, the precipitation rate, and the loss of snow to the ocean by the drifting snow mechanism. Since in the Northern Hemisphere the ice cover is generally thick and the snow cap is seasonal, the Arctic sea ice is not very sensitive to these variations. By contrast, the Antarctic ice pack, which is relatively thin and partly covered by perennial snow, is extremely responsive.

The contribution of sublimation to the surface mass balance of the sea-ice cover is potentially important. It can decrease the effective snow-accumulation rate by as much as 0.03 and 0.07 m of snow per month in the Arctic and Antarctic, respectively. Nevertheless, these figures probably overestimate the role of sublimation, since it is likely that a large part of the evaporative losses is returned back to the surface after condensation in the atmosphere. The actual relevance of this process could only be determined by the coupling of the model to an atmospheric model able to compute the moisture-holding capacity of the surface air layer.

The modelled snow–sea-ice system in the Arctic is rather insensitive to changes in the rate of precipitation. Large decreases in precipitation lead only to mild increases in the fall–winter ice volume, which result from the reduced thermal insulation of snow, while the summer ice cover remains virtually unaffected. It must be remembered, however, that the upper-ocean salinities in our model are relaxed towards annual mean observations and that a model without such artificial constraint could, in response to the perturbations in the freshwater flux, produce significant changes in the sensible heat flux to the ice. In the Southern Hemisphere, decreasing the precipitation does not modify much the total sea-ice volume. Nevertheless, a reduction of 50% in precipitation rate leads to an almost complete stoppage of snow-ice formation. The loss of ice volume due to the weakening of the latter process is, however, mostly compensated by an increase in the rate of basal ice accretion. An increase in precipitation has a more dramatic effect. The volumes of snow, ice, and snow-ice lagerly increase for precipitation rates 50% larger than that at present. This suggests that, in the Antarctic, the more active snow-ice formation induced by increasing snow accumulation can largely outpower the growing thermal insulation provided by the thickening snow. This finding goes against that of Eicken et al. (1995), who obtained an opposite response to increasing precipitation, which they attributed to the weakening of the conductive heat flux through ice. Obviously, it is still unclear which snow and ice processes and properties dominate the final mass balance of the Antarctic ice cover, and further investigation is needed. Given the high sensitivity of the Antarctic sea-ice cover to perturbations in precipitation, a realistic representation of the seasonal cycle of the snow, ice, and snow-ice covers in the Southern Ocean requires an accurate prescription of the precipitation rate. In this respect, it is worrying that the few climatologies of precipitation for the Antarctic available to date differ largely from one another. For example, the two widespread data sets of

Jaeger (1976), employed in this study, and of Legates and Willmott (1990) show discrepancies in the zonally averaged, monthly mean precipitation of more than 100% south of 60 °S. The use of the climatology of Legates and Willmott (1990) in our model leads to an increase in annual mean ice volume of about 23% with respect to our control value.

The influence of the blowing snow process on the net snow accumulation and on the freshwater balance of the mixed layer has been studied by using an admittedly crude approach. It has been shown that drifting snow is probably not a decisive factor for determining the seasonal cycle of sea-ice volume. But, it certainly directly affects the mass balance of the snow cover and, indirectly, that of snow ice.

We have also found in all experiments significant differences in the regional response of the Antarctic sea ice. As a general rule, the relatively thick and heavily snow-laden ice in the western Southern Ocean (particularly that in the Bellingshausen–Amundsen Seas) is far more responsive to the mentioned perturbations than its east Antarctic counterpart.

We caution that our results are liable to be modified if the experiments were repeated with a coupled climate model or even with a fully prognostic snow–sea-ice–ocean model. Modifications could arise, for example, because of the response of the atmosphere to variations in surface albedo (albedo–temperature feedback) and surface heat and evaporative fluxes, or the response of the oceanic heat flux to alterations in the surface freshwater balance. There are also some improvements that could be made in the snow, ice, and snow-ice parametrisations and that would add to the realism of the simulations. Among them, one may cite the use of time- and depth-dependent salinity, density, and thermal conductivity for snow and ice and of a surface albedo that evolves with the age and liquid-water content of snow and ice, the inclusion of an explicit snow-ice layer, and the introduction of mechanisms of snow-ice formation other than gravitational snow flooding (see Sect. 1).

The most important conclusion to be drawn from this work is that the Antarctic sea-ice cover is potentially very sensitive to variations in the rate of precipitation. Particularly, an increase in snowfall conduces to a parallel increase in total ice volume and area. This has important implications for the response of the Antarctic ice cover to enhanced greenhouse-gas concentrations. Model projections of global change show large increases in temperature over polar regions and an associated decay of the sea-ice cover. Concurrently, an increase in precipitation at high latitudes is also predicted (Houghton et al. 1996; Ye and Mather 1997). As long as surface air temperatures remain below freezing during part of the year, an increase in snow accumulation is expected to occur. Our results suggest that, in the Southern Ocean, the thickening of the snow cover would stimulate net ice growth via an enhancement of snow-ice formation, thus counteracting to some extent the effects of raising temperatures.

Acknowledgements We are grateful to K. Arrigo, H. Eicken, M. Jeffries and M. Leppäranta for their help and useful comments. We also thank H. Goosse for helpful discussions about various aspects of this work. The constructive criticisms of two anonymous reviewers have helped us to improve both the form and content of this paper, for which we are also grateful. T. Fichefet is a Research Associate at the National Fund for Scientific Research (Belgium). M. A. Morales Maqueda is a British Antarctic Survey (Natural Environment Research Council, United Kingdom) postdoctoral research fellow. This work was done within the scope of the Global Change and Sustainable Development Programme (Belgian State, Prime Minister's Services, Federal Office for Scientific, Technical, and Cultural Affairs, contract CG/DD/09A), the Concerted Research Action 092/97–154 (French Community of Belgium, Department of Education, Research, and Formation), and the Environment and Climate Programme (European Commission, contract ENV4–CT95–0102). All of this support is gratefully acknowledged.

References

Allison I, Brandt RE, Warren SG (1993) East Antarctic sea ice: albedo, thickness distribution, and snow cover. J Geophys Res 98 : 12417–12429

Andreas EL, Ackley ST (1982) On the differences in ablation seasons of Arctic and Antarctic sea ice. J Atmos Sci 39 : 440–447

Andreas EL, Makshtas AP (1985) Energy exchange over Antarctic sea ice in the spring. J Geophys Res 90 : 7199–7212

Arrigo KR, Worthen DL, Lizotte MP, Dixon P, Dieckmann G (1997) Primary production in Antarctic sea ice. Science 276 : 394–397

Barry RG, Serreze MC, Maslanik JA, Preller RH (1993) The Arctic sea ice–climate system : observations and modeling. Rev Geophys 31 : 397–422

Bourke RH, Garrett RP (1987) Sea ice thickness distribution in the Arctic Ocean. Cold Reg Sci Technol 13 : 259–280

Budd WF (1991) Antarctica and global change. Clim Change 18 : 272–299

Ebert EE, Curry JA (1993) An intermediate one-dimensional thermodynamic sea ice model for investigating ice-atmosphere interactions. J Geophys Res 98 : 10085–10109

Eicken H, Lange MA, Hubberten H-W, Wadhams P (1994) Characteristics and distribution patterns of snow and meteoric ice in the Weddell Sea and their contribution to the mass balance of sea ice. Ann Geophys 12 : 80–93

Eicken H, Fischer H, Lemke P (1995) Effects of the snow cover on Antarctic sea ice and potential modulation of its response to climate change. Ann Glaciol 21 : 369–376

Fichefet T, Morales Maqueda MA (1997) Sensitivity of a global sea ice model to the treatment of ice thermodynamics and dynamics. J Geophys Res 102 : 12,609–12,646

Gordon AL, Huber BA (1990) Southern Ocean winter mixed layer. J Geophys Res 95 : 11655–11672

Grenfell TC, Perovich DK (1984) Spectral albedos of sea ice and incident solar irradiance in the southern Beaufort Sea. J Geophys Res 89 : 3573–3580

Hanson AM (1965) Studies of the mass budget of Arctic pack-ice floes. J Glaciol 5 : 701–709

Harvey LDD (1988) Development of a sea ice model for use in zonally averaged energy balance climate models. J Clim 1 : 1221–1238

Holland DM, Mysak LA, Manak DK, Oberhuber JM (1993) Sensitivity study of a dynamic thermodynamic sea ice model. J Geophys Res 98 : 2561–2586

Houghton JT, Meira Filho LG, Callander BA, Harris N, Kattenberg A, Maskell K (eds) (1996) Climate change 1995. The science of climate change. Cambridge University Press, Cambridge, UK, 572 pp

Jacka TH, Allison I, Thwaites R, Wilson JC (1987) Characteristics of the seasonal sea ice of East Antarctica and comparisons with satellite observations. Ann Glaciol 9 : 85–91

Jaeger L (1976) Monatskarten des niederschlags für die ganze Erde. Ber Deutsch Wetterdienstes 139, 38 pp

Jeffries MO, Adolphs U (1997) Early winter ice and snow thickness distribution, ice structure and development of the western Ross Sea pack ice between the ice edge and the Ross Ice Shelf. Antarctic Sci 9 : 188–200

Jeffries MO, Shaw RA, Morris K, Veazey AL, Krouse HR (1994a) Crystal structure, stable isotopes (δ^{18}O), and development of sea ice in the Ross, Amundsen, and Bellingshausen seas, Antarctica. J Geophys Res 99 : 985–995

Jeffries MO, Veazey AL, Krouse HR (1994b) Depositional environment of the snow cover on West Antarctic pack-ice floes. Ann Glaciol 20 : 33–38

Jeffries MO, Worby AP, Morris K, Weeks WF (1997) Seasonal variations in the properties and structural composition of the sea ice and snow cover in the Bellingshausen and Amundsen Seas, Antarctica. J Glaciol 43 : 138–151

Lange MA, Eicken H (1991) The sea ice thickness distribution in the northwestern Weddell Sea. J Geophys Res 96 : 4821–4837

Lange MA, Schlosser P, Ackley SF, Wadhams P, Dieckmann GS (1990) ^{18}O concentrations in sea ice of the Weddell Sea, Antarctica. J Glaciol 36 : 315–323

Ledley TS (1985) Sensitivity of a thermodynamic sea ice model with leads to time step size. J Geophys Res 90 : 2251–2260

Ledley TS (1991) Snow on sea ice: competing effects in shaping climate. J Geophys Res 96 : 17195–17208

Ledley TS (1993) Variations in snow on sea ice: a mechanism for producing climate variations. J Geophys Res 98 : 10401–10410

Legates DR, Willmott CJ (1990) Mean seasonal and spatial variability in gauge-corrected, global precipitation. Int J Climatol 10 : 111–127

Leppäranta M (1983) A growth model for black ice, snow ice and snow thickness in subarctic basins. Nordic Hydrol 14 : 59–70

Lytle VI, Ackley SF (1996) Heat flux through sea ice in the western Weddell Sea: convective and conductive transfer processes. J Geophys Res 101 : 8853–8868

Male DH, Granger RJ (1981) Snow surface energy balance. Water Resour Res 17 : 609–627

Massom RA, Drinkwater MR, Haas C (1997) Winter snow cover on sea ice in the Weddell Sea. J Geophys Res 102 : 1101–1117

Maykut GA, Untersteiner N (1971) Some results from a time-dependent thermodynamic model of sea ice. J Geophys Res 76 : 1550–1575

Mellor M, Fellers G (1986) Concentration and flux of wind-blown snow. Cold Regions Research and Engineering Laboratory SP 86–11, Hanover, 20 pp

Morales Maqueda MA (1995) Un Modelo Acoplado del Hielo de Mar y del Océano Superficial para Estudios Climáticos. PhD thesis, Universidad Complutense de Madrid, 426 pp

Neeman BU, Joseph JH, Ohring G (1988) A vertically integrated snow/ice model over land/sea for climate studies. J Geophys Res 93 : 3663–3675

Owens WB, Lemke P (1990) Sensitivity studies with a sea ice–mixed layer–pycnocline model in the Weddell Sea. J Geophys Res 95 : 9527–9538

Scharfen G, Barry RG, Robinson DA, Kukla G, Serreze MC (1987) Large-scale patterns of snow melt on Arctic sea ice mapped from meteorological satellite imagery. Ann Glaciol 9 : 200–205

Semtner AJ (1976) A model for the thermodynamic growth of sea ice in numerical investigations of climate. J Phys Oceanogr 6 : 379–389

Shine KP, Henderson-Sellers A (1985) The sensitivity of a thermodynamic sea ice model to changes in surface albedo parametrization. J Geophys Res 90 : 2243–2250

Stössel A, Lemke P, Owens WB (1990) Coupled sea ice-mixed layer simulations for the Southern Ocean. J Geophys Res 95 : 9539–9555

Takahashi T (1960) On the puddles of Lützow-Holm Bay. In: Dwyer LJ (ed) Antarctic meteorology. Pergamon Press, Oxford, England, pp 317–332

Vowinckel E, Orvig S (1970) The climate of the North Polar Basin. In: Orvig S (ed) Climates of the Polar Regions. World Survey of Climatology, vol 14, Elsevier, Amsterdam, The Netherlands, pp 129–252

Wadhams P, Lange MA, Ackley SF (1987) The ice thickness distribution across the Atlantic sector of the Antarctic Ocean in midwinter. J Geophys Res 92 : 14,535–14,552

Weatherly JW, Walsh JE (1996) The effects of precipitation and river runoff in a coupled ice–ocean model of the Arctic. Clim Dyn 12 : 785–798

Worby AP, Jeffries MO, Weeks WF, Morris K, Jaña R (1996) The thickness distribution of sea ice and snow cover during late winter in the Bellingshausen and Amundsen Seas, Antarctica. J Geophys Res 101 : 288441–28455

Ye HC, Mather JR (1997) Polar snow cover changes and global warming. Int J Climatol 17 : 155–162